# Supplementary Materials: Primary Human Renal Proximal Tubular Epithelial Cells (pHRPTEpiCs): Shiga Toxin (Stx) Glycosphingolipid Receptors, Stx Susceptibility and Interaction with Membrane Microdomains

**Johanna Detzner, Anna-Lena Klein, Gottfried Pohlentz, Elisabeth Krojnewski, Hans-Ulrich Humpf, Alexander Mellmann, Helge Karch and Johannes Müthing**
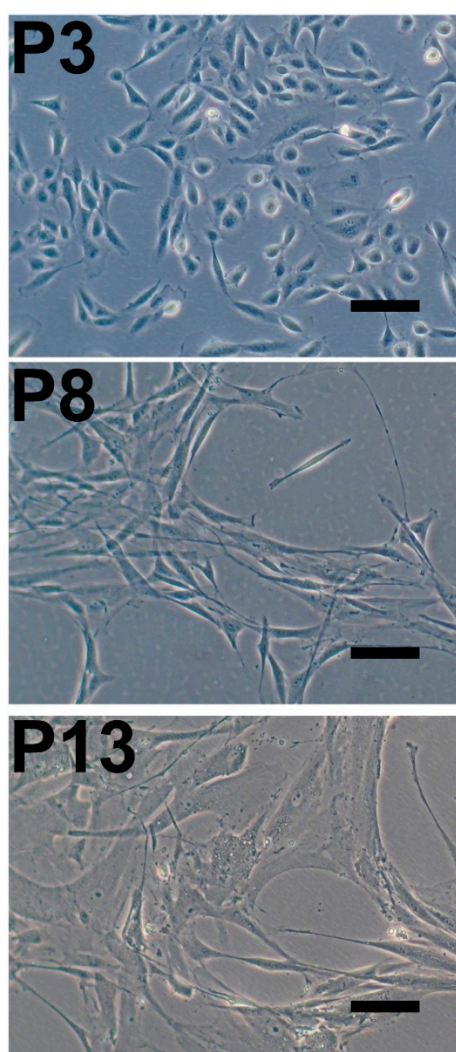
**Figure S1.** Light microscopy micrographs of pHRPTEpiCs during passage 3 (**P3**), passage 8 (**P8**), and passage 13 (**P13**) at approximate 30% confluence. Original magnification ×10. Bar: 100 μm.
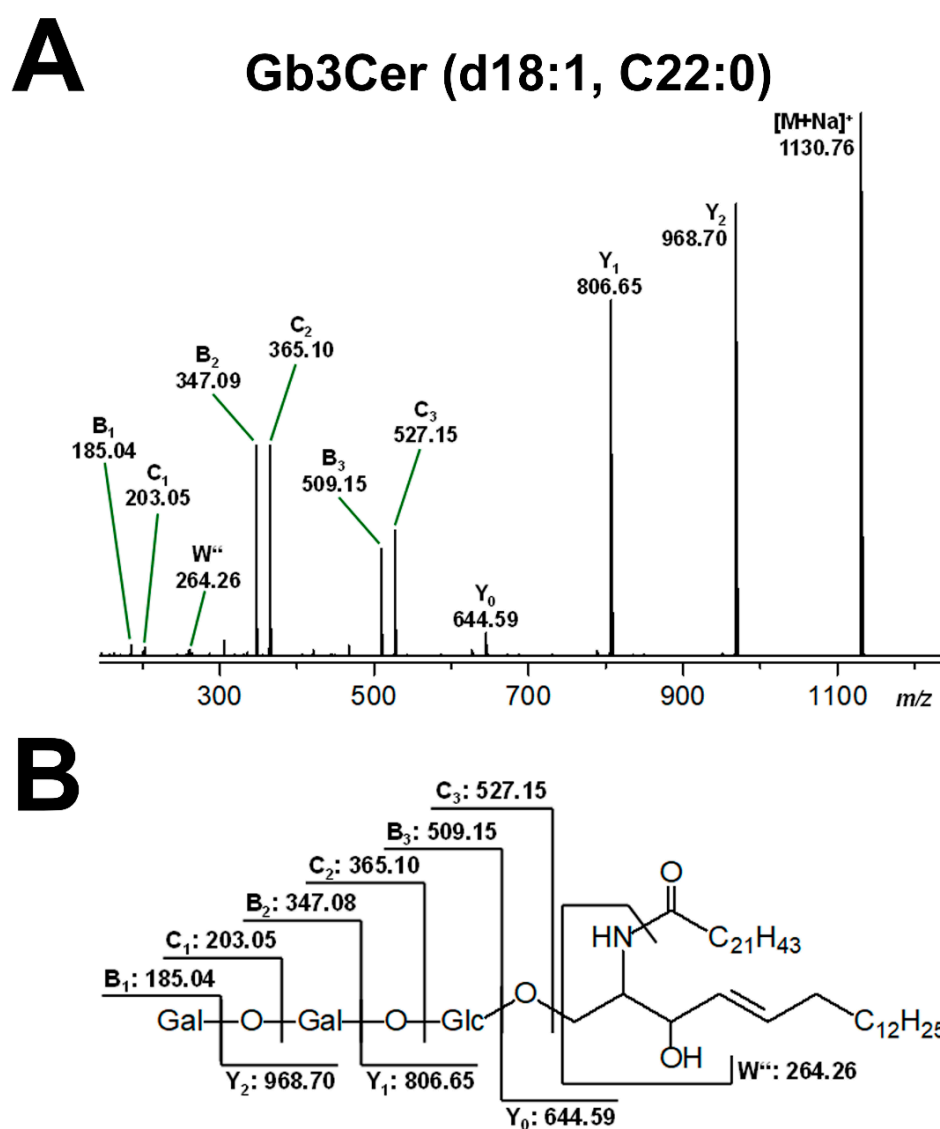
**Figure S2.** MS$^2$ spectrum of Gb3Cer (d18:1, C22:0) (**A**) and corresponding fragmentation scheme (**B**) obtained from pHRPTEpiCs.
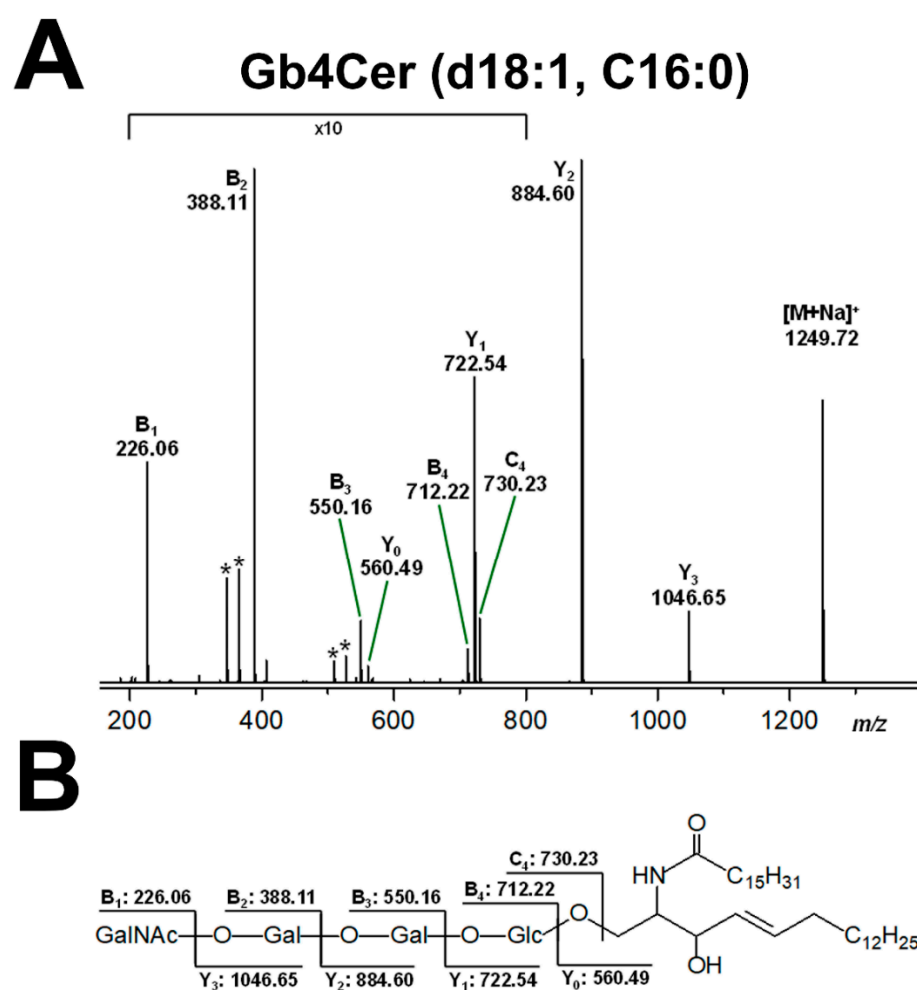
**Figure S3.** MS$^2$ spectrum of Gb4Cer (d18:1, C16:0) (**A**) and corresponding fragmentation scheme (**B**) obtained from pHRPTEpiCs.
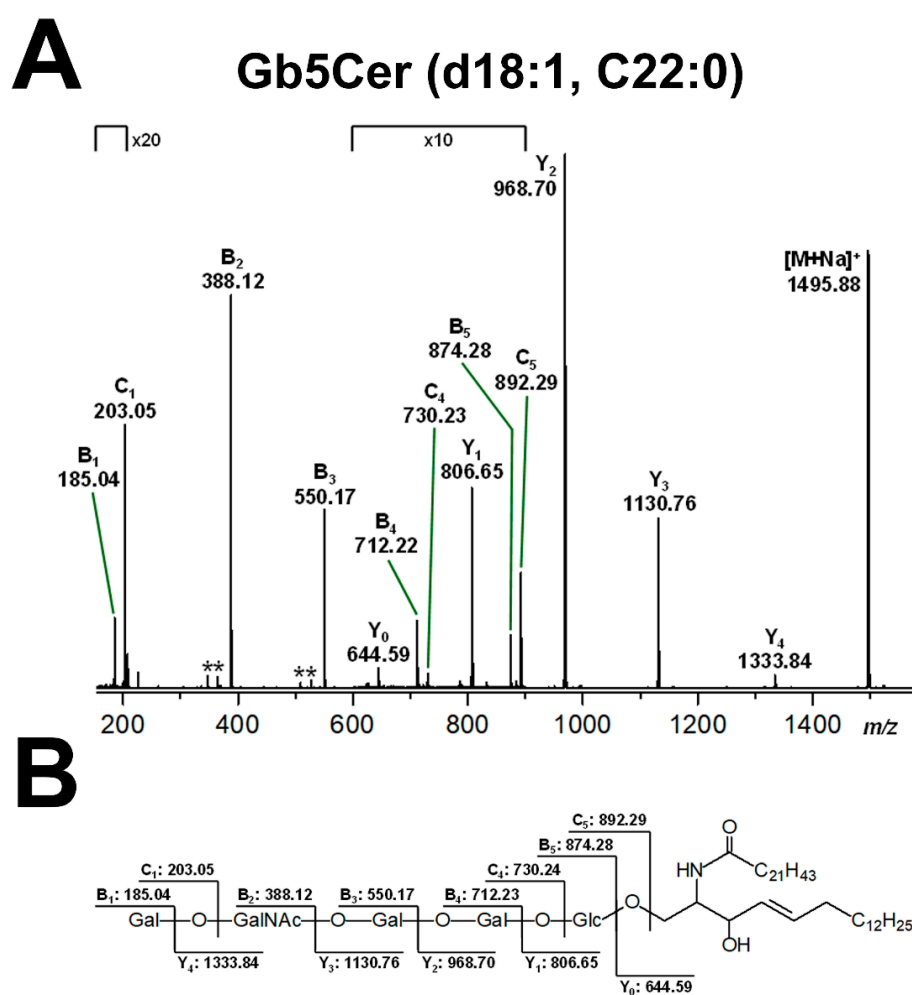
**Figure S4.** MS$^2$ spectrum of Gb5Cer (d18:1, C22:0) (**A**) and corresponding fragmentation scheme (**B**) obtained from pHRPTEpiCs.
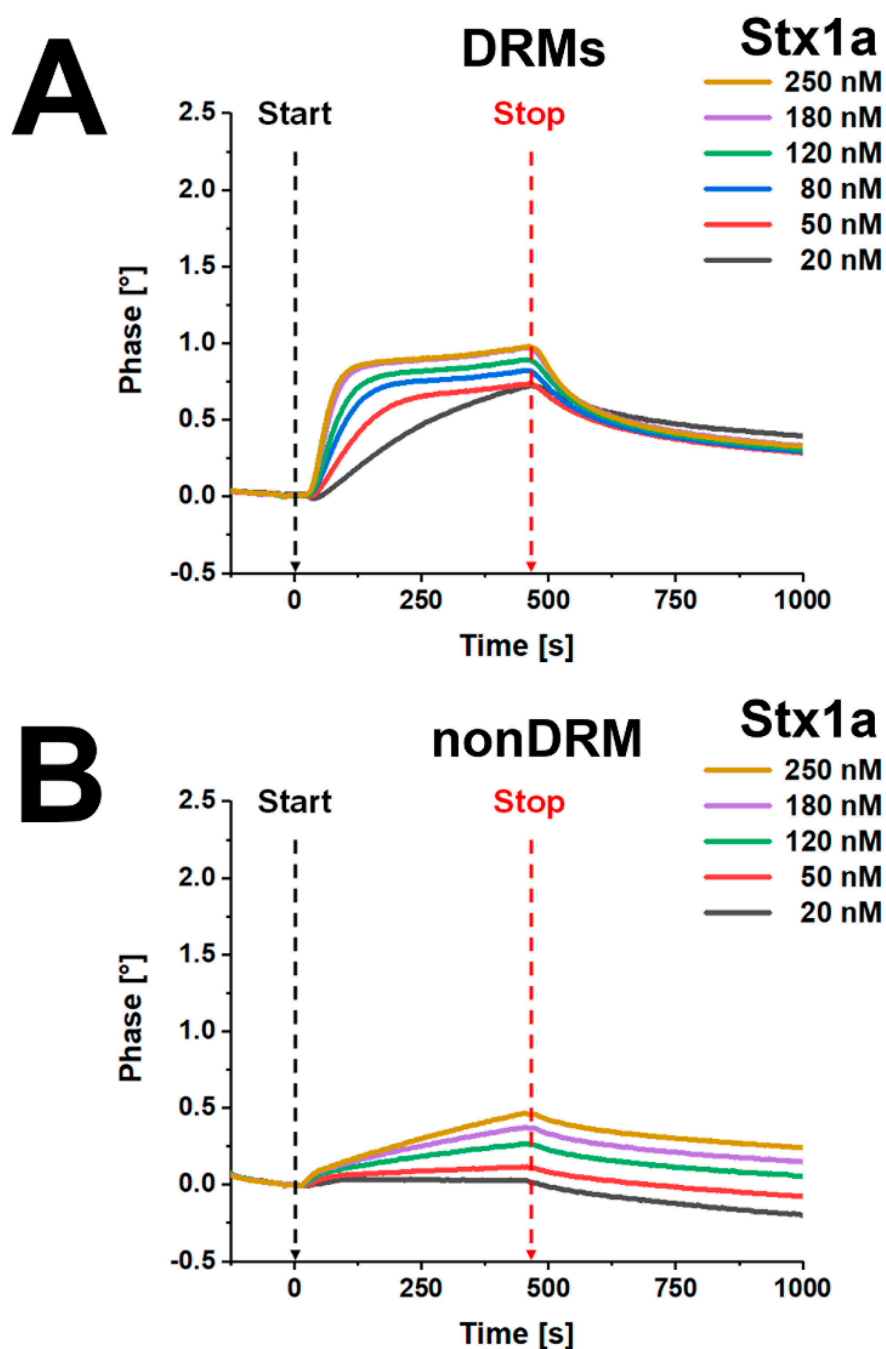
**Figure S5.** SAW real-time interaction sensorgrams gained for binding of Stx1a towards DRM (**A**) and nonDRM fractions (**B**) prepared from replicate 1 of pHRPTEpiCs.
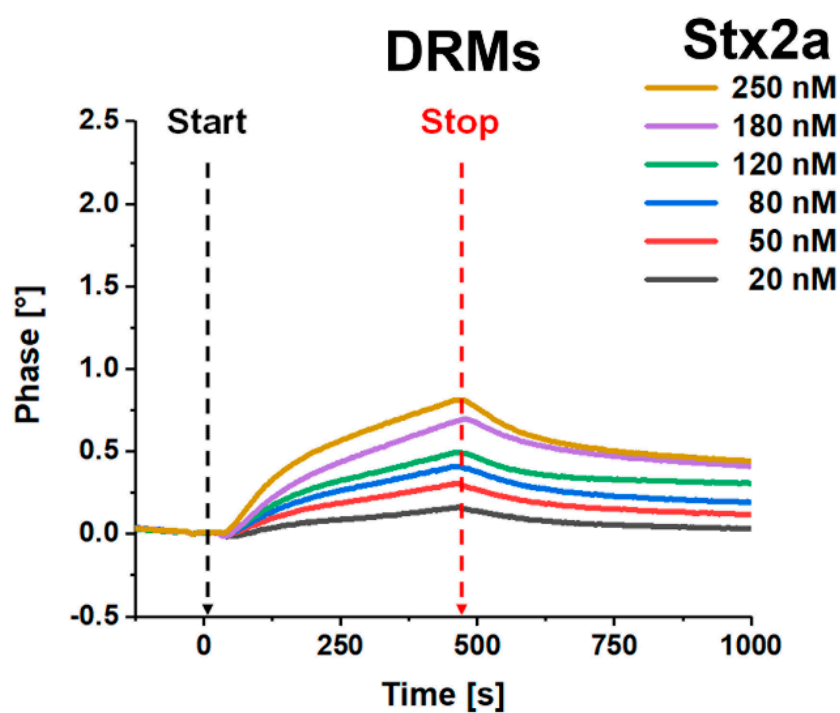
**Figure S6.** SAW real-time interaction sensorgrams gained for binding of Stx2a towards DRM fractions prepared from replicate 1 of pHRPTEpiCs.

**Table S1.** Relative distribution of Gb3Cer, Gb4Cer, and cholesterol in sucrose gradient fractions obtained from pHRPTEpiCs.

**Gb3Cer**

| Fraction | Replicate 1 (%) | | Replicate 2 (%) | |
|---|---|---|---|---|
| F1 DRM (top) | 0.0 | | 14.8 | |
| F2 DRM (top) | 49.6 | | 48.9 | |
| F3 DRM (top) | 16.4 | Σ66.0 (F1–F3) | 14.1 | Σ77.8 (F1–F3) |
| F4 nonDRM (intermediate) | 7.7 | | 8.1 | |
| F5 nonDRM (intermediate) | 8.9 | | 5.4 | |
| F6 nonDRM (intermediate) | 8.4 | Σ25.0 (F4–F6) | 0.0 | Σ13.5 (F4–F6) |
| F7 nonDRM (bottom) | 7.0 | | 7.7 | |
| F8 nonDRM (bottom) | 2.0 | Σ9.0 (F7–F8) | 1.0 | Σ8.7 (F7–F8) |
| | | Σ100.0 (F1–F8) | | Σ100.0 (F1–F8) |

**Gb4Cer**

| Fraction | Replicate 1 (%) | | Replicate 2 (%) | |
|---|---|---|---|---|
| F1 DRM (top) | 0.0 | | 10.1 | |
| F2 DRM (top) | 64.9 | | 59.1 | |
| F3 DRM (top) | 15.9 | Σ80.8 (F1–F3) | 11.7 | Σ80.9 (F1–F3) |
| F4 nonDRM (intermediate) | 5.4 | | 5.9 | |
| F5 nonDRM (intermediate) | 5.0 | | 2.1 | |
| F6 nonDRM (intermediate) | 3.8 | Σ14.2 (F4–F6) | 0.0 | Σ8.0 (F4–F6) |
| F7 nonDRM (bottom) | 5.0 | | 9.8 | |
| F8 nonDRM (bottom) | 0.0 | Σ5.0 (F7–F8) | 1.3 | Σ11.1 (F7–F8) |
| | | Σ100.0 (F1–F8) | | Σ100.0 (F1–F8) |

**Cholesterol**

| Fraction | Replicate 1 [%] | | Replicate 2 [%] | |
|---|---|---|---|---|
| F1 DRM (top) | 0.0 | | 4.8 | |
| F2 DRM (top) | 57.4 | | 47.5 | |
| F3 DRM (top) | 13.3 | Σ70.7 (F1–F3) | 14.9 | Σ67.2 (F1–F3) |
| F4 nonDRM (intermediate) | 6.1 | | 9.3 | |
| F5 nonDRM (intermediate) | 9.0 | | 7.8 | |
| F6 nonDRM (intermediate) | 5.3 | Σ20.4 (F4–F6) | 0.0 | Σ17.1 (F4–F6) |
| F7 nonDRM (bottom) | 7.5 | | 14.1 | |
| F8 nonDRM (bottom) | 1.4 | Σ8.9 (F7–F8) | 1.6 | Σ15.7 (F7–F8) |
| | | Σ100.0 (F1–F8) | | Σ100.0 (F1–F8) |

**Table S2.** Calculated association $k_{ass}$ and dissociation $k_{diss}$ rate constants and equilibrium dissociation constant $K_D$ for Stx1a using DRMs of pHRPTEpiCs[a.]

| Sensor channel | $k_{ass}$ (nM$^{-1}$ s$^{-1}$)[b] | $k_{diss}$ (s$^{-1}$)[b] | $K_D$ (nM)[b] |
|---|---|---|---|
| 1 | $1.0 \times 10^{-4}$ | $8.8 \times 10^{-3}$ | 88.3 |
| 2 | $1.0 \times 10^{-4}$ | $8.2 \times 10^{-3}$ | 81.8 |
| 3 | $1.0 \times 10^{-4}$ | $7.4 \times 10^{-3}$ | 73.9 |
| 4 | $0.9 \times 10^{-4}$ | $6.9 \times 10^{-3}$ | 76.2 |
| 5 | $0.8 \times 10^{-4}$ | $6.2 \times 10^{-3}$ | 77.5 |
| Mean value | $0.9 \times 10^{-4}$ | $7.5 \times 10^{-3}$ | 79.5 |
| SD[c] | $8.9 \times 10^{-6}$ | $1.0 \times 10^{-3}$ | 5.7 |

[a] Constants were determined by real-time interaction analysis of Stx1a with sensor surface-coated pooled DRM fractions F1-F3 prepared from replicate 1 of pHRPTEpiCs; [b] $k_{ass}$, $k_{diss}$ and $K_D$ values were obtained for Stx1a and correspond to sensorgrams of Figure 12; [c] SD, standard deviation.